

RESEARCH ARTICLE

Artificial spider silk supports and guides neurite extension in vitro

Magnus L. Hansson^{1,2}  | Urmimala Chatterjee¹ | Juanita Francis¹ | Tina Arndt¹  | Christian Broman² | Jan Johansson¹ | Mattias K. Sköld^{2,3}  | Anna Rising^{1,4} 

¹Department of Biosciences and Nutrition, Karolinska Institutet, Huddinge, Sweden

²Experimental Traumatology Unit, Department of Neuroscience, Biomedicum B8 Karolinska Institutet, Stockholm, Sweden

³Department of Neuroscience, Section of Neurosurgery, Uppsala University, Uppsala, Sweden

⁴Department of Anatomy, Physiology and Biochemistry, Swedish University of Agricultural Sciences, Uppsala, Sweden

Correspondence

Mattias K. Sköld, Experimental Traumatology Unit, Department of Neuroscience, Biomedicum B8 Karolinska Institutet, S-171 77 Stockholm, Sweden.
Email: mattias.skold@ki.se

Anna Rising, Department of Biosciences and Nutrition, Karolinska Institutet, Neo, 141 86 Huddinge, Sweden.
Email: anna.rising@ki.se

Funding information

EC | European Research Council (ERC), Grant/Award Number: 815357; The Center for Innovative Medicine at Karolinska Institutet and Stockholm City Council, Karolinska Institutet SFO Regen, Grant/Award Number: FOR 4-1364/2019; Swedish Research Council, Grant/Award Number: 2019-01257

Abstract

Surgical intervention with the use of autografts is considered the gold standard to treat peripheral nerve injuries. However, a biomaterial that supports and guides nerve growth would be an attractive alternative to overcome problems with limited availability, morbidity at the site of harvest, and nerve mismatches related to autografts. Native spider silk is a promising material for construction of nerve guidance conduit (NGC), as it enables regeneration of cm-long nerve injuries in sheep, but regulatory requirements for medical devices demand synthetic materials. Here, we use a recombinant spider silk protein (NT2RepCT) and a functionalized variant carrying a peptide derived from vitronectin (VN-NT2RepCT) as substrates for nerve growth support and neurite extension, using a dorsal root ganglion cell line, ND7/23. Two-dimensional coatings were benchmarked against poly-D-lysine and recombinant laminins. Both spider silk coatings performed as the control substrates with regards to proliferation, survival, and neurite growth. Furthermore, NT2RepCT and VN-NT2RepCT spun into continuous fibers in a biomimetic spinning set-up support cell survival, neurite growth, and guidance to an even larger extent than native spider silk. Thus, artificial spider silk is a promising biomaterial for development of NGCs.

KEYWORDS

biomaterial, nerve guidance conduit, peripheral nerve, recombinant spider silk

Abbreviations: CNS, central nervous system; dbcAMP, N₆,2'-O-dibutyryladenine 3', 5'-cyclic monophosphate; DRG, dorsal root ganglion; ECM, extracellular matrix; hESC, human embryonic stem cells; hNPC, human neural progenitor cells; NGC, nerve guidance conduit; PDL, poly-D-lysine; PI, propidium iodide; PLA, polylactic acid; PNS, peripheral nervous system; RGD, Arginine-Glycine-Aspartic acid.

This is an open access article under the terms of the Creative Commons Attribution-NonCommercial-NoDerivs License, which permits use and distribution in any medium, provided the original work is properly cited, the use is non-commercial and no modifications or adaptations are made.

© 2021 The Authors. *The FASEB Journal* published by Wiley Periodicals LLC on behalf of Federation of American Societies for Experimental Biology

1 | INTRODUCTION

Injuries to the nervous system are a major medical problem, both in the peripheral nervous system (PNS) and the central nervous system (CNS).^{1,2} While there are very limited possibilities for nerve regrowth after injuries in the CNS the picture is different in the PNS.^{3,4} In the PNS, nerve autografts are considered the gold standard for treating nerve defects and are used on a regular basis.⁵ However, the success of such nerve conduits varies substantially and aspects such as location and type of nerve, the proximity of the injury and age at injury all have an impact on the capacity for the injured nerve to regenerate. In addition, limited availability and loss of function at the donor site restrict the use of autografts.^{6,7} Therefore, development of artificial nerve guidance conduits (NGCs) with biodegradable and biocompatible properties is considered a promising alternative to nerve autografts.^{8–11}

The extracellular matrix (ECM) plays several crucial roles in the development, regeneration, and maintenance of the PNS¹² and may be of value for engineering NGCs. Laminins are prominent components of the ECM in the PNS and have been shown to support axon growth as well as Schwann cell migration *in vitro* and *in vivo*.^{13,14} Laminins are trimeric and composed of α , β , and γ glycoproteins. The different laminin isoforms are named after their chain composition, for example, laminin-111 (L111) contains $\alpha 1$, $\beta 1$, and $\gamma 1$ chains, and laminin-521 (L521) consists of $\alpha 5$, $\beta 2$, and $\gamma 1$ chains.¹⁵ Laminins interact with cell membrane receptors such as integrins, syndecans, and dystroglycans as well as with growth factors and other ECM proteins.¹⁶ Another important ECM protein is vitronectin, which interacts with integrin receptors $\alpha\beta 5$ and $\alpha\beta 1$ on the cell surface via its Arg-Gly-Asp (RGD) motif.¹⁷ Vitronectin has been shown to support outgrowth of hippocampal neurites *in vitro* and vitronectin loaded on to polylactic acid (PLA) substrates efficiently increases neurite growth and branching of mouse cortical neurons.^{18,19} Additionally, an RGD containing peptide derived from vitronectin has successfully been used for long-term xeno-free expansion of both human embryonic stem cells (hESCs) and human neural progenitor cells (hNPCs) with subsequent cardiomyocyte and neuronal differentiation, respectively.^{20,21}

Spider silk possesses several features of a material intended for NGCs, such as high strength, extensibility, good biocompatibility, and biodegradability.²² Furthermore, native spider silk has successfully been used to bridge 6-cm-long peripheral nerve injuries in animal models.^{23,24} From a clinical point of view, however, recombinant spider silk would be superior to the natural fiber since it is of non-animal origin and contains only a single defined protein in contrast to the natural fiber that is composed of many different proteins.

Production of proteins in heterologous systems also comes with the benefit of allowing modifications of the produced proteins, such as covalently incorporated functional motifs.^{25–30} Hence, recombinant spider silk fibers could both provide physical guidance for sprouting neurites as has been described for the native fiber, and be decorated with cell binding motifs providing signals that promote neurite extension. In addition to the relatively straightforward and feasible manufacturing process of recombinant spider silk fibers, such a scaffold would potentially outcompete those made from, for example, vitronectin only since it cannot be spun into fibers and likely be more flexible and bioactive compared to fibers manufactured from synthetic polymers. We have previously shown that recombinant spider silk can be functionalized by introducing a vitronectin derived peptide in the N-terminus of the recombinant spider silk protein 4RepCT (VN-4RepCT) and coatings made from this protein are suitable for long-term proliferation of human pluripotent stem cells (hPSCs) under chemically defined conditions.^{29,31} Unfortunately, limitations such as low yield and poor solubility in water of the 4RepCT³² and VN-4RepCT have hindered further development of these proteins. Recently, we engineered a miniature spider silk protein (NT2RepCT) that can be produced at large amounts in *Escherichia coli*.³³ NT2RepCT recapitulates the high solubility of native spider silk proteins (can be concentrated to 50% w/v), display viscoelastic rheological properties^{33,34} and can be spun into continuous fibers in a biomimetic spinning procedure.³³ This opens up the possibility of using fibers made from NT2RepCT (and variants thereof carrying e.g., cell binding motifs) as scaffolds for nerve regeneration.

Here, we functionalize the recombinant spider silk protein NT2RepCT with a covalently linked vitronectin peptide (VN-NT2RepCT). These two recombinant spider silk proteins were used to make coatings that were evaluated as cell culture substrates against three different recombinant laminins and poly-D-lysine (PDL). The different coatings were evaluated in terms of proliferation, survival, and neurite outgrowth of a neuronal cell line ND7/23, which is a fusion of neonatal rat dorsal root ganglion neurons and N18tg2 mouse neuroblastoma cells. Fibers spun from NT2RepCT and VN-NT2RepCT were benchmarked against fibers collected from the Swedish bridge spider (*Larinioides sclopetarius*) in terms of neurite extension and guidance.

2 | MATERIAL AND METHODS

2.1 | Protein expression and purification

The mini-spidroin NT2RepCT was produced as previously described.³⁵ To incorporate an integrin binding motif from

vitronectin in NT2RepCT, the sequence encoding the amino acid sequence PQVTRGDVFTLP was cloned into the pT7-6xHis-NT2RepCT construct following the 6xHis-tag. In brief, the plasmids pT7-6xHis-NT2RepCT and pT7-VN-6xHis-NT2RepCT were transformed into *E. coli* BL21DE3 and stored as glycerol stocks. From the glycerol stocks, precultures in Luria broth (LB) media with kanamycin (70 mg/L) were inoculated and grown overnight at 37°C with shaking (220 rpm). One liter of LB media with kanamycin (70 mg/L) was inoculated with 10 ml preculture and grown at 30°C with shaking (110 rpm) until the optical density at 600 nm (OD_{600}) reached 0.8 after which the temperature was lowered to 20°C. Protein expression was induced by adding isopropylthiogalactoside (IPTG) to a final concentration of 0.3 mM. Cell culturing continued overnight at 20°C with shaking (110 rpm) and then cells were harvested (20 min at 7278 g, 4°C). The pellets were resuspended in 20 mM Tris-HCl pH 8. Cells were lysed with a cell disrupter (T-S Series Machine, Constant Systems Limited, England) at 30 kPsi and the lysate was centrifuged at 27 000 g, 4°C for 30 min. Affinity chromatography purification was performed under gravity flow conditions by subjecting the supernatant of the lysate to Ni-NTA columns as previously stated³⁵ or by using an Äkta start chromatography system and HisPrep FF 16/10 (Cytiva) ready-to-use columns. The Äkta start system was first equilibrated in 20 mM Tris pH 8. The supernatant was loaded onto the column at a flow rate of 5 ml/min and subsequently washed with 20 mM Tris-HCl pH 8 and 2 mM imidazole. For both methods, the desired proteins were eluted with 300 mM imidazole. The eluted protein was dialyzed against 20 mM Tris-HCl pH 8, at 4°C overnight. The purity of the protein was validated by SDS-PAGE. The protein was concentrated to 300 mg/ml using centrifugal filter units (Vivaspin 20, GE healthcare) with a 10 kDa molecular weight cutoff at 4000 g in rounds of 20 min. The protein concentration was determined from absorbance at 280 nm.

2.2 | Spinning fibers and making coated films

Fiber spinning was performed as previously described³⁵ with slight modifications. Round glass capillaries (G1, Narishige) with an outer diameter of 1.0 mm and inner diameter of 0.6 mm were pulled (Micro Electrode Puller, Stoelting co. 51217) to a tip diameter of 40–50 μ m. A 1 ml syringe with Luer Lok tip (BD) was filled with NT2RepCT or VN-NT2RepCT with a concentration (300 mg/ml) and connected to a 27G steel needle (Braun) with an outer diameter of 0.40 mm. The needle was connected to the pulled glass capillary via polyethylene tubing. A neMESYS low

pressure (290N) syringe pump (Cetoni) was used to extrude the NT2RepCT at a flow rate of 17 μ l/min into a low pH spinning buffer (500 mM acetate buffer and 200 mM NaCl). As the fibers were extruded out of the capillary, they were guided along the collection bath using a 1 μ l inoculation loop. At the end of the bath, the fibers were collected onto glass chamber slides (SPL Life Sciences Co., Ltd. 30104/30108) fitted onto six rotating diapositive slide frames mounted on a motorized wheel. The fibers on the glass slides were removed from the wheel and incubated overnight in the low pH spinning buffer in petri dishes. The spinning buffer was removed and sterile phosphate-buffered saline (PBS, pH 7) was added to the fibers and left to incubate for 1 h at room temperature. After incubation in PBS the fibers on the glass slides were removed from the buffer and sterilized under UV light. The chamber slide walls were then applied, and the fibers were secured to the bottom of the chamber slides. For collecting natural spider silk from a Swedish bridge spider (*L. sclopetarius*), the spider was first anesthetized with CO₂ and then placed onto a wax plate. The spider was gently pinned down to immobilize it, without injuring the animal. The dragline silk was extruded from the anterior spinneret.³⁶ Aided by a Zeiss Stemi 305 stereo microscope the silk from the anterior spinneret was gently pulled out with the help of a tweezer and was collected onto glass chamber slides fitted onto six rotating diapositive slide frames mounted on a motorized wheel at 7.5 m/min. The silk was collected for a few minutes in this way until the spider stopped producing it.

Two-dimensional coatings of NT2RepCT and VN-NT2RepCT were made on 24-well plates (Thermo Scientific, 142475). Two hundred and fifty microliters of the protein solution at a concentration of 0.1 mg/ml containing 2.5 mg/ml D(+) Glucono delta-lactone and 1/6 of the total volume of 20 mM HEPES buffer was added to each well and incubated at room temperature for 1 h. The excess protein solution was removed from the wells and the plates were incubated overnight at 37°C for drying. The plates were then sterilized under UV light and used for cell culture experiments.

To verify that silk proteins remained in the wells after coating, 100 μ l of a 0.1 mg/ml NT2RepCT solution (sterile filtered and unfiltered) was used to coat a 48-well plate (Costar 3548, Corning) as described above. For one set of samples the protein solution was removed and the wells were dried as mentioned before. For the other set of samples the protein solution was let to dry without removing the excess liquid. Fifty microliters of SDS buffer was added to each well and the plate was shaken for 1 h at room temperature. The solutions were removed from each well, boiled and subjected to SDS gel electrophoresis.

2.3 | Laminins and PDL coatings

Human recombinant laminins (BioLamina AB, Sweden) were coated in empty wells or onto spider silk coatings following BioLamina instructions. Shortly, laminin-111 and laminin-511 stock solutions were diluted in 1×DPBS ($\text{Ca}^{2+}/\text{Mg}^{2+}$) to a final concentration of 5 $\mu\text{g}/\text{ml}$ and 300 $\mu\text{l}/\text{well}$ were added in a 24-well plate. For laminin-521, a concentration of 10 $\mu\text{g}/\text{ul}$ was used for the coatings, in accordance to the manufacturer's instructions. The laminin solutions were incubated at 37°C for 4 h, and the protein solution was removed. Coatings of laminin blends were performed as described above and scaled down proportionally in order to keep the total amount of laminins constant: 300 $\mu\text{l}/\text{well}$ of each laminin blend were used for the coatings with the following concentrations: L111+L511 blend with a final concentration of 5 $\mu\text{g}/\text{ml}$ (2.5 μg of L111 and 2.5 μg L511 per ml), L111+L521 blend: 2.5 $\mu\text{g}/\text{ml}$ of L111 and 5 $\mu\text{g}/\text{ml}$ of L521; L511+L521 blend: 2.5 $\mu\text{g}/\text{ml}$ of L511 and 5 $\mu\text{g}/\text{ml}$ of L521; L111+L511+L521: 1.67 + 1.67 + 3.33 $\mu\text{g}/\text{ml}$.

For poly-D-lysine (PDL) coatings, 100 μl of 0.1 mg/ml PDL (Thermo Fisher Scientific) were added to the wells and incubated at room temperature for 5 min and thereafter rinsed thoroughly with sterile tissue culture grade water and dried for 2 h at room temperature.

2.4 | Cell culture

ND7/23 cells (Sigma-Aldrich), an immortalized fusion cell line of DRG neonatal rat neuron and mouse neuroblastoma cells, were cultured in Duplecco's modified Eagle's medium (DMEM) supplemented with 100 U/ml penicillin, 100 mg/ml streptomycin (Sigma-Aldrich) and 10% fetal bovine serum (FBS) (Thermo Fisher Scientific).

For proliferation, cells were seeded at a density of 5000 cells/ cm^2 and at different time points (24, 48, and 72 h), the cells were detached by trypsin and diluted in media with trypan blue. The number of dead and live cells were then counted by Countess Automated Cell Counter (Invitrogen). The cell number at different time points were calculated as fold increase to seeding density (0 h).

2.5 | Neurite growth on coatings

Cells were resuspended in DMEM + 0.5% FBS to a concentration of 18 000 cells/ml and then seeded into 24-well plates and incubated at 37°C for 20 h to inhibit mitosis. The next day, neurite outgrowth was induced by adding differentiation media, DMEM + 0.5% containing 1mM dbcAMP (N6,2'-O-Dibutyryl adenosine 3',5'-cyclic

monophosphate) (D0627, Sigma-Aldrich), and incubated for additionally 48 h.

2.6 | Neurite growth on fibers

Four-well or 8-well chamber slides (SPL Life Sciences Co., Ltd. 30104/30108) with NT2RepCT, VN-NT2RepCT or native spider silk were washed with DMEM two times with 30 min incubation at 37°C between each wash. ND7/23 cells were resuspended with DMEM + 0.5% FBS and 1% Penicillin/Streptomycin and seeded into chamber slides with density of 7000 cells/ cm^2 . After approximately 20 h incubation, the media were replaced with differentiation media and incubated at 37°C for additional 48 h.

2.7 | Live dead staining of differentiating cells

After 48 h of dbcAMP treatment, the media were removed and 0.5 ml of pre-warmed fresh media containing 1 μM of Calcein-AM (Sigma-Aldrich) were added to each well and the plates were incubated at 37°C for 30 min. To stain for cell nucleus and dead cells 1 drop of Hoechst3342 and 1 drop of Propidium Iodide (PI) were added into each well (NucBlue Live reagent, Thermo Fisher scientific). Cell survival was calculated as a percentage of green cells to the total cell number (Hoechst3342 positive, blue). In experiments where PI was included the cell viability was validated by counting the number of PI stained cells and calculating the percentage of dead cells (PI positive cells, red). PI staining was later on excluded since the results from the Calcein-AM/Hoechst-3342 matched very well with the results obtained from PI/Hoechst33-42 and Calcein-AM/PI (i.e., cells co-stained with PI/Hoechst (dead cells) were not Calcein-AM positive and cells co-stained with Calcein-AM/Hoechst3342 (live cells) were not PI positive).

2.8 | Phalloidin- and immunostaining

The ND7/23 cells were fixed with paraformaldehyde 3.7% (w/v) for 15 min at room temperature, permeabilized with 0.1% Triton X-100 (Sigma-Aldrich) for 15 min and blocked for 40 min with 5% bovine serum albumin (BSA). Antibodies were diluted in 1% BSA in PBS containing 0.01% Tween-20. Tubulin β primary antibodies (diluted 1:1000; Sternberger, SMI61) were then added and incubated for 2 h. Secondary antibodies and Phalloidin-Atto (diluted 1:50, Sigma-Aldrich) were counterstained for 30 min at room temperature. Coverslips were mounted

using Vectashield mounting medium with DAPI (4',6-diamidino-2-phenylindole (VectorLabs).

2.9 | Imaging and image analysis

All bright field (BF) images were captured automatically with the Cell-IQ (Chipman technologies). The fluorescence images were captured in an inverted microscope (Axio Observer, Zeiss). Dead, live, and total number of cells were counted by using Image J software (NIH).

Neurite outgrowth and the longest neurite length per neuron was measured using Neuron J (ImageJ plug-in, NIH). Neurite outgrowth was evaluated by counting cells with neurites that were longer than the cell body. More than 100 cells per well and three wells per type of coating from at least three independent experiments were analyzed.

2.10 | Western blotting

To verify efficient coating of laminins in the plates (Figure S2), the coating procedure was performed as described above. After removing unbound laminins, the coatings were solubilized by addition of SDS-PAGE sample loading buffer (5×) containing β -mercaptoethanol (5%), transferred into tubes and boiled for 5 min and spun for 5 min at 11 000 rpm. Proteins were electrophoresed through 4%–20% polyacrylamide gels and transferred to polyvinylidene difluoride (PVDF) 0.2 μ m transfer membranes (Amersham, Hybond). Membranes were blocked with 10% skim milk for 1 h at room temperature and incubated with LAMC1 primary antibody (1:1000; Sigma-Aldrich) at 4°C overnight. After 4 × 5 min washes in phosphate-buffered saline and 0.1% tween 20 (PBST), the membrane was treated with horseradish peroxidase-linked donkey antimouse IgG (1:5000; GE Healthcare) for 1 h at room temperature. Followed by 4 × 5 min washings in PBST, the membranes were developed with Amersham ECL Prime western blotting detection reagent kit.

2.11 | Statistics

Statistical analyses were performed in GraphPad Prism 8.0 (La Jolla California USA, www.graphpad.com). One-way ANOVA (analysis of variance) followed by Tukey's post hoc tests, Dunnett's post hoc tests, or Sidak's multiple comparison tests. *p* values of <.05 were considered as significant.

3 | RESULTS

3.1 | Design of a functionalized spider silk protein

We engineered a functionalized variant of NT2RepCT by introducing an N-terminally linked integrin binding motif derived from vitronectin (VN-NT2RepCT; Figure 1B). The VN-NT2RepCT protein was overexpressed in *E. coli* and was recovered from the soluble fraction of the cell lysate by affinity chromatography (Figure S1). The yield was 21 mg/L using the same conditions as previously described for NT2RepCT.

3.2 | Growth rate, cell viability, and neurite outgrowth of ND7/23 cells on different coatings

To investigate the proliferation and survival of ND7/23 cells on NT2RepCT and VN-NT2RepCT, we coated cell culture plates with the spider silk proteins, and for comparison, included PDL and Laminin-111 (L111), Laminin-511 (L511), and Laminin-521 (L521) coatings. The presence of the silk protein after coating was verified by solubilizing the coating followed by SDS-PAGE analysis (Figure S2). ND7/23 cells were seeded onto the different matrices and were followed over time. The cells attached to the substrates and proliferated well on all coatings (Figure 1A), displaying a uniform distribution which supports that all coatings covered the bottom of the wells. As the cells grew toward confluency, they occasionally grew on top of each other in multilayered structures. This is in line with the manufacturer's description of the cell line and conforms to previous reports in which the cells were cultured on PDL, plastic, or glass surfaces.³⁷ However, in the L511 and L521 coated wells, the cells continued to grow as monolayers, also toward confluency, which suggests more efficient adhesion to the substrate (Figure 1A). The rate of the cell growth was similar for all coatings with no significant differences (Figure 1C). Importantly, trypan blue staining revealed that the cell survival over time was high for all coatings, including NT2RepCT and VN-NT2RepCT (>75%; Figure 1D), with highest values for VN-NT2RepCT (91%), L111 (91%), or L511 (93%). These results show that ND7/23 cells efficiently expand on NT2RepCT and VN-NT2RepCT coated surfaces.

Next, we investigated to what extent the different coatings affected the neurite outgrowth. Cells were seeded in 24-well plates with different coatings as described above and after an overnight incubation in low serum media, neurite outgrowth was stimulated by addition of dbcAMP for 48 h, whereafter the cells were stained and visualized

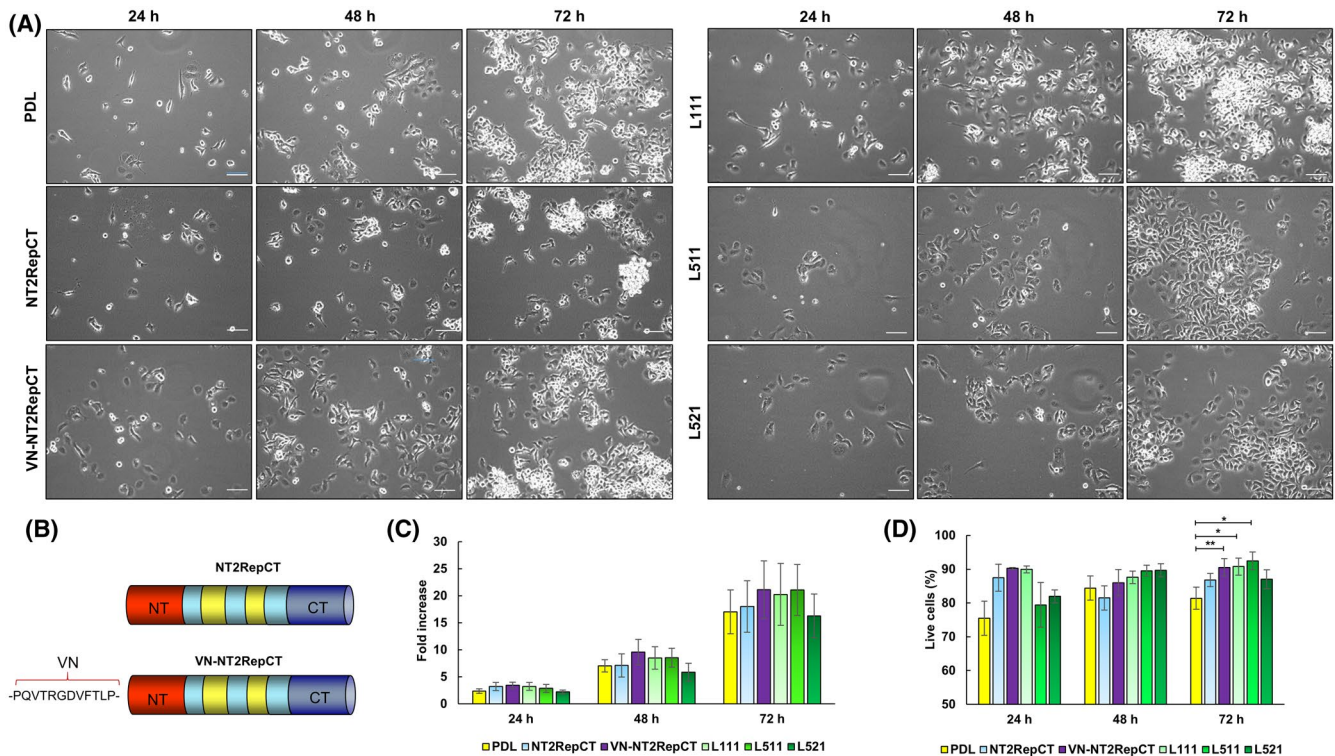


FIGURE 1 ND7/23 cell proliferation and viability on PDL, NT2RepCT, VN-NT2RepCT, L111, L511, and L521. The cells were seeded in 24-well plates with different coatings and phase contrast micrographs of proliferating ND7/23 cells were taken at 24, 48, and 72 h (A). Schematic illustration of NT2RepCT and VN-NT2RepCT (B). Growth analyzed by trypan blue staining and subsequent cell counting and percentage live cells after 24, 48, and 72 h (C and D). Data are presented as mean \pm SEM from at least two independent experiments performed in duplicates or triplicates. Statistically significant differences were analyzed by ANOVA mixed model and Tukey's post hoc test. * $p < .05$ and ** $p < .01$. Scale bar: 100 μm , applies to all panels in (A)

under a fluorescence microscope (Figure 2A). The fractions of live cells were between 75% and 85% with no significant differences between the coatings (Figure 2B). The fraction of neurite-bearing cells was on average 28% on PDL coatings, which is in line with the results from cells cultured on NT2RepCT or VN-NT2RepCT (26% and 35%, respectively; Figure 2C). In contrast, only 16% and 19% of cells cultured on L521 or L511, respectively, had neurites which were significantly lower than for the cells cultured on VN-NT2RepCT. The mean neurite length was approximately 1.4-fold longer for cells cultured on L521 compared with PDL coatings, and approximately 1.7- and 1.3-fold longer compared to NT2RepCT and VN-NT2RepCT, respectively (Figure 2D). Neurites from cells grown on L511 coatings were significantly longer than those from cells grown on PDL and NT2RepCT coatings. There were no significant differences in the mean neurite length for cells growing on PDL, NT2RepCT, VN-NT2RepCT, and L111. Next, we analyzed the 10% longest neurites for all coatings (Figure 2E) and found that the 10% longest neurites were $93 \pm 21 \mu\text{m}$ for NT2RepCT and $133 \pm 14 \mu\text{m}$ for VN-NT2RepCT ($p < .05$). For the cells on PDL, L111, L511, and L521 the 10% longest neurites were all between 105 and 110 μm . Thus, cells grown on NT2RepCT and

VN-NT2RepCT develop neurites to the same or larger extent compared to cells on the control substrates. The average length of neurites was comparable, except for L511 and L521 that supported longer but fewer neurites. When quantifying the length of the 10% longest neurites in the cultures, the VN-NT2RepCT coating performed best.

3.3 | Neurite outgrowth on laminins and laminin blends coated on top of VN-NT2RepCT

Since VN-NT2RepCT coatings resulted in the highest percentage of cells with neurites which also were relatively long, and L511 and L521 had long neurites but fewer cells with neurites, we hypothesized that coating of laminins on top of VN-NT2RepCT could improve the growth of the neurites further. To investigate this, ND7/23 cells were seeded in plates that were coated with single laminins (L111, L511, or L521) or laminin mixtures (i.e., L111+L511, L111+L521, L511+L521, or L111+L511+L521) on top of VN-NT2RepCT, or on laminin mixtures coated in the wells without VN-NT2RepCT. The cells were differentiated for 48 h by addition of dbcAMP, and then live

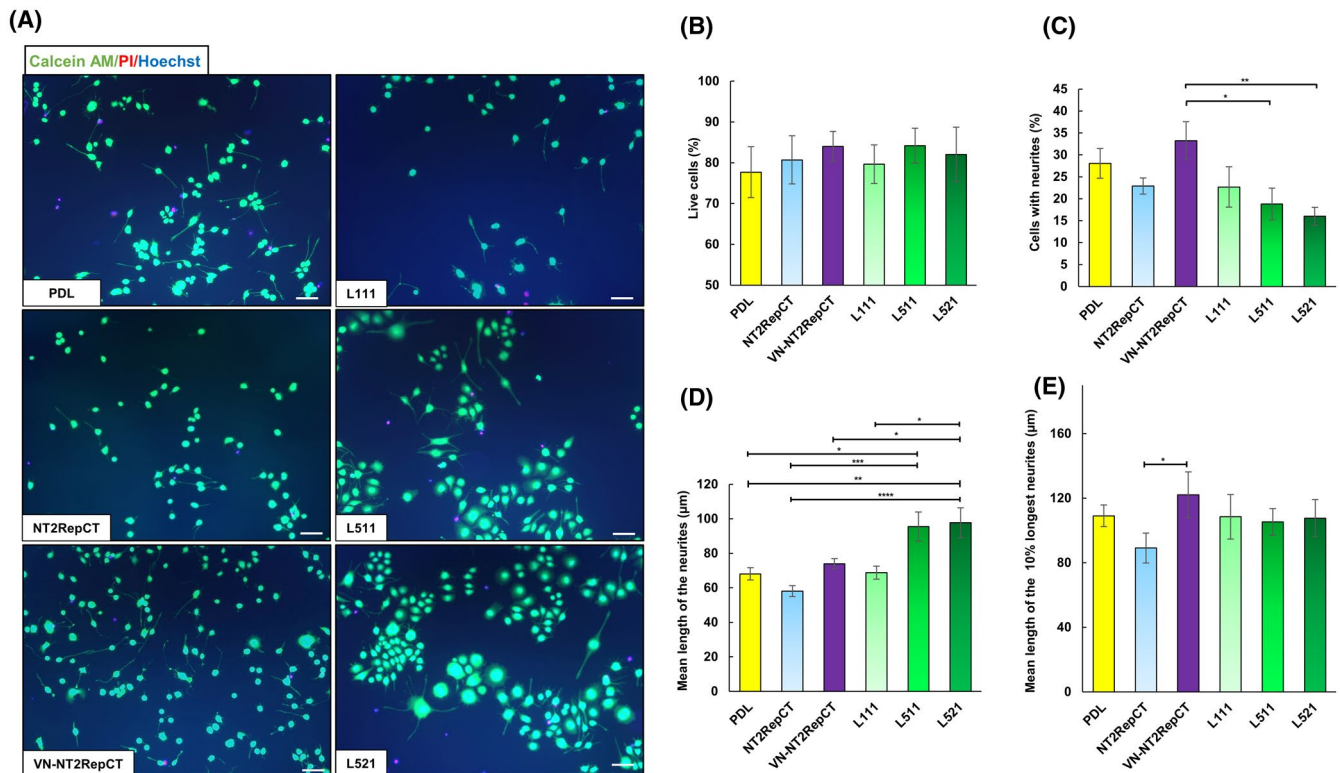


FIGURE 2 Neurite outgrowth and viability of ND7/23 cells differentiated on PDL, NT2RepCT, VN-NT2RepCT, L111, L511, and L521. Neurite outgrowth was induced by addition of 1 mM dibutyryl cyclic AMP (dbcAMP). Representative images of merged channels showing ND7/23 cells labeled with Calcein-AM, Hoechst, and propidium iodide (PI) 48 h after addition of dbcAMP (A). The cell survival after 48 h was assessed (B) and the percentage of cells bearing at least one neurite (C). The average length of the longest neurite per cell (D) and the 10% longest neurites/image (E). More than 100 cells per well were analyzed in triplicates and experiments were done three times. Data are presented as mean \pm SEM. Scale bar: 100 μ m, applies to all panels in (A)

stained and recorded under fluorescence microscope (Figure 3A). Analysis after differentiation revealed that between 75% and 90% of the cells were alive on all coatings (Figure 3B). None of the single laminins coated on top of VN-NT2RepCT improved the proportion of neurite-bearing cells compared to VN-NT2RepCT coatings. There was a tendency that laminins coated on top of VN-NT2RepCT resulted in larger fraction of cells with neurites than laminin coatings only (L521, 16% vs. VN-NT2RepCT+L521, 25%, $p < .05$, Figures 2C and 3C). Thus, none of the mixed laminin and VN-NT2RepCT coatings investigated outperformed the VN-NT2RepCT in terms of cell survival and fraction neurite-bearing cells.

Next, we analyzed the neurite length of cells growing on the different substrates. Analyses of the longest neurite per cell for cells on single laminin coatings on top of VN-NT2RepCT did not show any improvements in neurite lengths compared to those on PDL or VN-NT2RepCT, but neurites from cells that grew on a mixture with L511 and L521 coated on top of VN-NT2RepCT were approximately 1.5- and 1.4-fold longer than neurites on PDL and VN-NT2RepCT, respectively (Figure 3D). Analyses of the 10% longest neurites of cells cultured on single laminin coatings

on top of VN-NT2RepCT did not reveal any increase when compared to those on VN-NT2RepCT (Figure 3E). Regarding the laminin blends coated on top of VN-NT2RepCT, the 10% longest neurites of cells were grown on VN-NT2RepCT+L111+L521 or VN-NT2RepCT+L511+L521 matrices were significantly longer than neurites that grew on PDL. However, compared with VN-NT2RepCT matrices, we could not detect any significant increase in the length of the 10% longest neurites. Moreover, comparison of the different laminin blends versus the corresponding laminin blends coated on top of VN-NT2RepCT did not show any significant differences. These results suggest that the VN-NT2RepCT coatings per se efficiently support neurite outgrowth (proportion of cells with neurites) and elongation (length of the longest neurites) to the same degree as different combinations of laminins.

3.4 | Neurite outgrowth on artificial and natural spider silk fibers

While two-dimensional coatings are convenient for analyzing the behavior of cells on different substrates, fibers

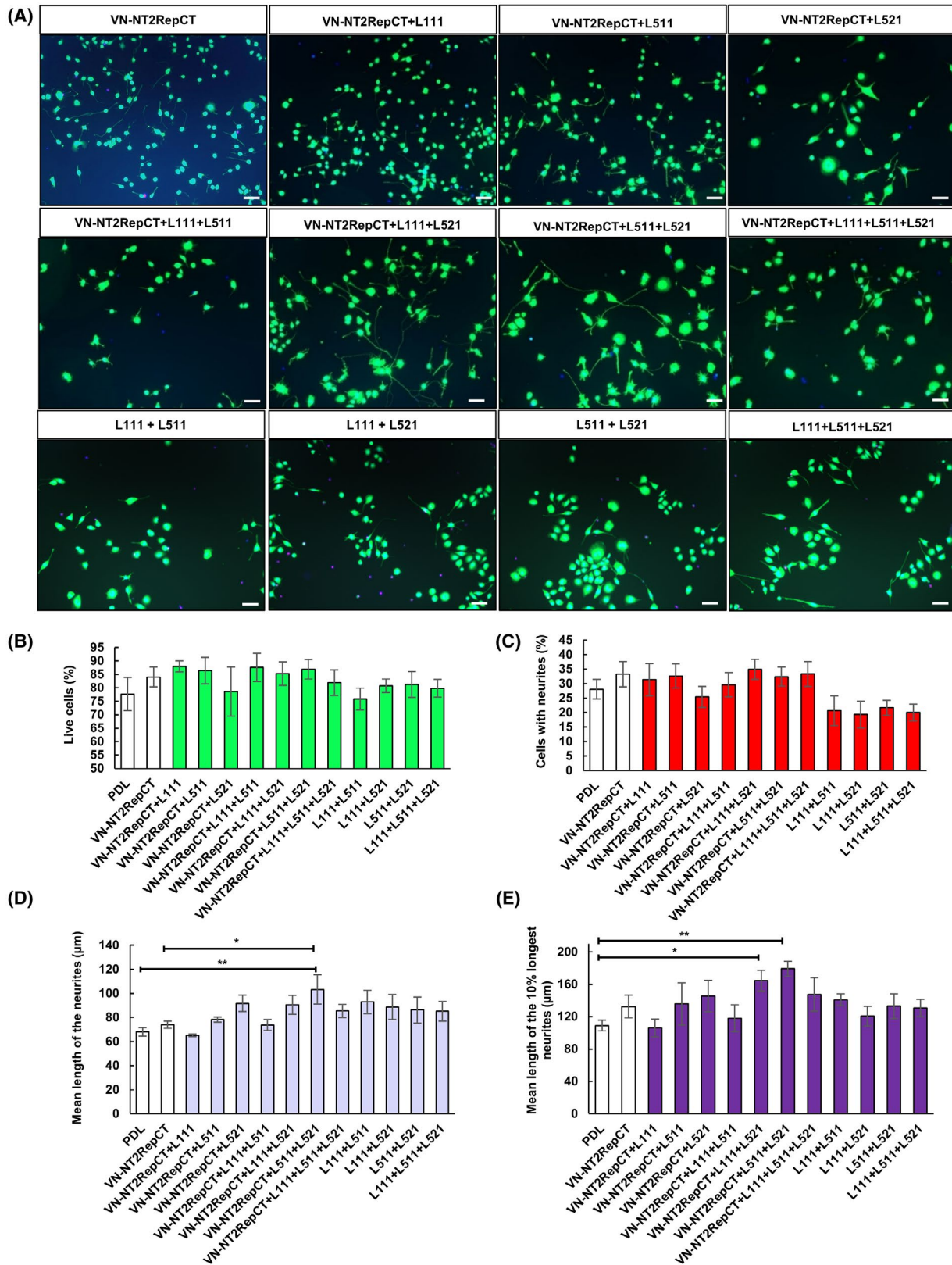


FIGURE 3 Viability and neurite outgrowth of ND7/23 cells on combined coatings. Representative images of merged channels showing ND7/23 cells labeled with 1 μ M Calcein-AM, Hoechst 33342 and PI (not included in all pictures) 48 h after addition of dbcAMP (A). The cell survival at 48 h was assessed by imageJ (B) and the percentage of cells bearing at least one neurite in NeuronJ (C). The average length of the longest neurite per cell (D) and the 10% longest neurites/image (E). 100–200 cells per well were analyzed in triplicates and experiments performed at least three times. White bars represent results from Figure 2. Data are presented as mean \pm SEM. Scale bar: 100 μ m, applies to all panels in (A)

would be ideal for making NGCs. We have previously shown that NT2RepCT, expressed in *E. coli* and purified to homogeneity, can be spun into fibers in a biomimetic spinning set-up.³³ Using the same conditions, VN-NT2RepCT could successfully be spun into continuous fibers (Figure 4A,B). To explore if NT2RepCT and/or VN-NT2RepCT fibers could promote cell adhesion and enable neurite growth and guidance, we used snap on chamber slides that allowed us to first collect silk fibers wrapped around a microscope slide, then secure the fibers by snapping on the well walls (Figure 4C). As a control, we collected natural spider silk from the Swedish bridge spider (*L. sclopetarius*) and mounted the silk on chamber slides in the same manner.

After seeding, the ND7/23 cells were treated with dbcAMP to activate neurite outgrowth (Figure 4D–F) using the same protocol as for the coatings. After 48 h differentiation, we stained live cells and determined the cell survival, which was between 70% and 75% on all fiber types (Figure 4G). Next, we determined the fraction of cells on the fiber that had neurites extending along the fiber axis, away from fiber, or along the fibers but not on the fibers (referred to as “parallel”), respectively (Figure 5A). Interestingly, most of the cells (69%) on NT2RepCT fibers grew their longest neurites on and along the fiber, whereas only 26% of their longest neurites grew away from the fiber. For cells cultured in the presence of VN-NT2RepCT fibers, approximately 44% extended their longest neurites on and along the fiber and 53% of the neurites grew away from the fiber. Analyses of cells cultured on native spider silk, revealed that only 21% of the longest neurites were extending on and along the fiber and that the majority of the neurites (70%) were growing away from the fibers. All three fiber types had a low percentage of cells with neurites growing in parallel with the fibers. In addition, we measured the length of the neurites for each fiber type and category described above. There was no difference in mean length when comparing neurites growing along NT2RepCT ($74 \pm 15 \mu\text{m}$), VN-NT2RepCT ($56 \pm 6 \mu\text{m}$), or native fibers ($56 \pm 6 \mu\text{m}$) (Figure 5C). We also analyzed cells with the cell body placed at a distance from the fiber but that had neurites in physical contact with the fibers (Figure 5D). In these analyses, the cells were separated in three categories: those with a neurite growing toward-on fiber, neurite growing toward-on and along fiber, and neurite growing toward-on and away from the fiber (Figure 5D). The highest fraction of neurites for all three fiber types were found in the toward-on group. Interestingly, the neurites growing toward the native silk fiber continued across the fiber to a larger extent than those growing toward the artificial silk fibers (Figure 5E), suggesting that the artificial fibers may be superior in guiding sprouting neurites.

Finally, in order to visualize the neurite growth on the fibers at higher magnifications, the cultures were fixed and stained with tubulin antibody to reveal microtubules in the neurites and phalloidin to reveal the microfilaments in the cells. (Figure 5F–H).

4 | DISCUSSION

The use of biomaterials as nerve guidance conduits (NGCs) holds great promise to improve the clinical outcome of traumatic nerve injuries, but there is a lack of materials that can outperform autologous nerve grafts. Spider silk is an interesting biomaterial for nerve regeneration that in several studies using large animal models of critically sized nerve defects have shown excellent ability to mediate regeneration of peripheral nerves.^{23,24,38} However, for clinical applications, a chemically defined material is needed. Previously, we developed NT2RepCT that can be produced at high yields and can be spun into continuous fibers using extrusion of a 300 mg/ml NT2RepCT solution into a pH 5 aqueous buffer. This was the first process for continuous biomimetic fiber spinning of recombinant silk proteins,³³ a requirement for the development of NGCs.

To improve the performance of biomaterials, different bioactive molecules or parts thereof, can be added in the manufacturing process, for example, ECM proteins,^{39–41} functional peptides,^{42–45} neurotrophic factors,^{46,47} small molecules,^{48,49} or miRNA.^{50,51} One such example is a peptide derived from vitronectin that was shown to support expansion of undifferentiated hESCs and hNPCs.^{20,21} This peptide has also been used to functionalize a spider silk protein (VN-4RepCT) which resulted in a substrate for efficient culture and passage of human pluripotent stem cells^{29,31} but problems with low yield and lack of methods for spinning continuous fibers prevented further development of this material.³² Against this background, we decided to design a functionalized variant of NT2RepCT that carries a RGD containing vitronectin motif N-terminally (VN-NT2RepCT) and explore its ability to promote cell survival and neurite extension. The yields of VN-NT2RepCT were high, the protein was extremely soluble in aqueous buffers, and we could spin it into fibers in the same manner as NT2RepCT (Figure 4A,B). Thus, the presence of the VN peptide N-terminally did not negatively affect the solubility or spinnability of the protein, which was not evident considering that dimerization of the N-terminal domain is key to the fiber formation and since changes in primary structure can affect the morphology and properties of protein fibrils.^{33,52–54}

In this study, we used a DRG cell line (ND7/23) as a model to study cell survival and neurite extension.

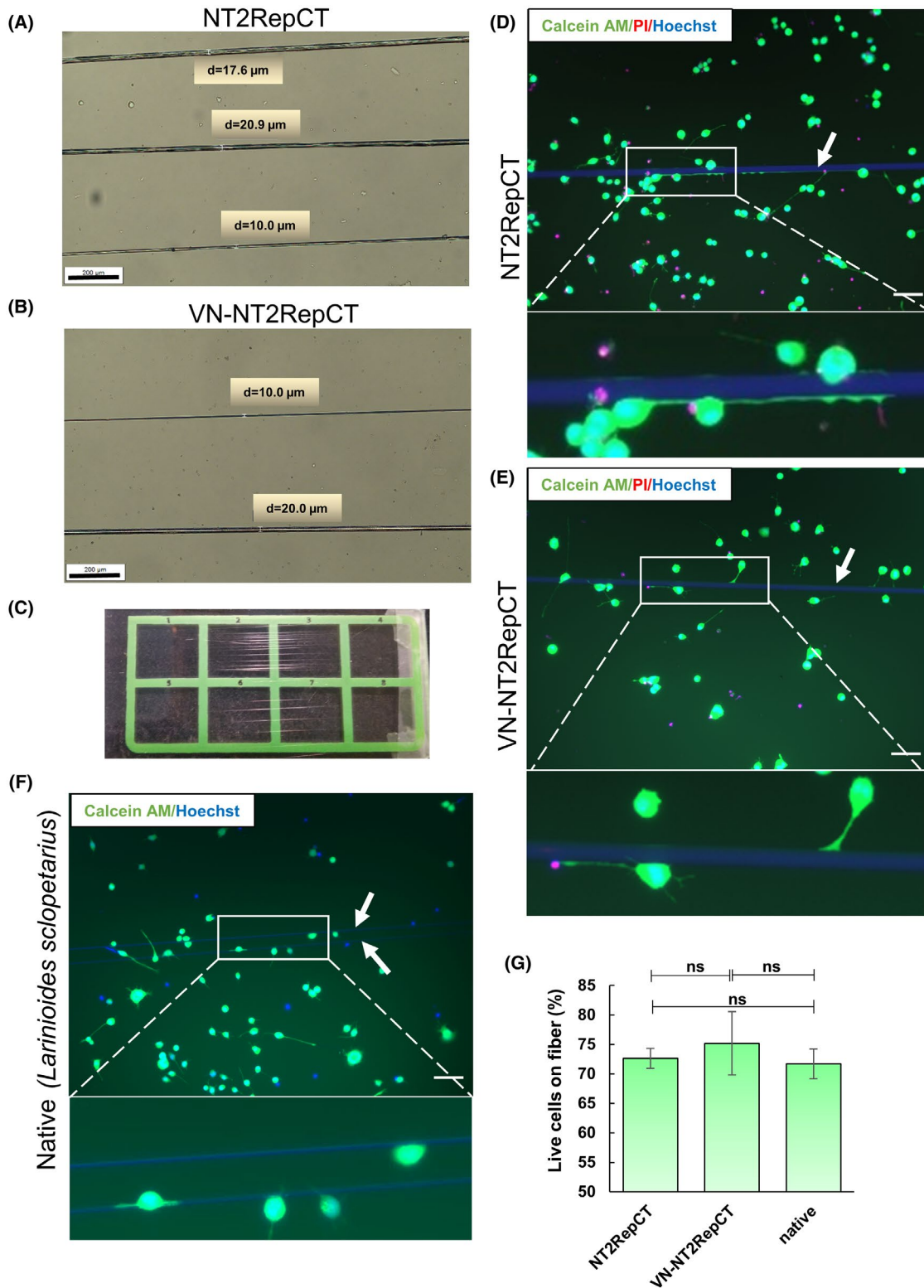


FIGURE 4 Cell survival of differentiating ND7/23 cells cultured on artificial and native spider silk. Representative micrographs on NT2RepCT (A) and VN-NT2RepCT (B) fibers, where the diameter (d) of the fibers was measured at indicated sites. Aligned fibers attached to a slide (C). Representative images of merged channels showing ND7/23 cells differentiated for 48 h on NT2RepCT (D), VN-NT2RepCT (E), and native spider silk from *Larinioides scolopetarius* (F). The cells were labeled with Calcein-AM (green), Hoechst3342 (blue) and PI (red) (not included in the image with native silk) dyes. Cell survival on the three different fiber types were calculated as a percentage of green cells to the total cell number (blue) (G). Data represent mean \pm SEM. NT2RepCT and VN-NT2RepCT were performed in five independent experiments and native spider silks were analyzed from four independent experiments. ns, not significant. Scale bars: 200 μm applies to (B) and (C), and 100 μm applies to upper panels of (D–F)

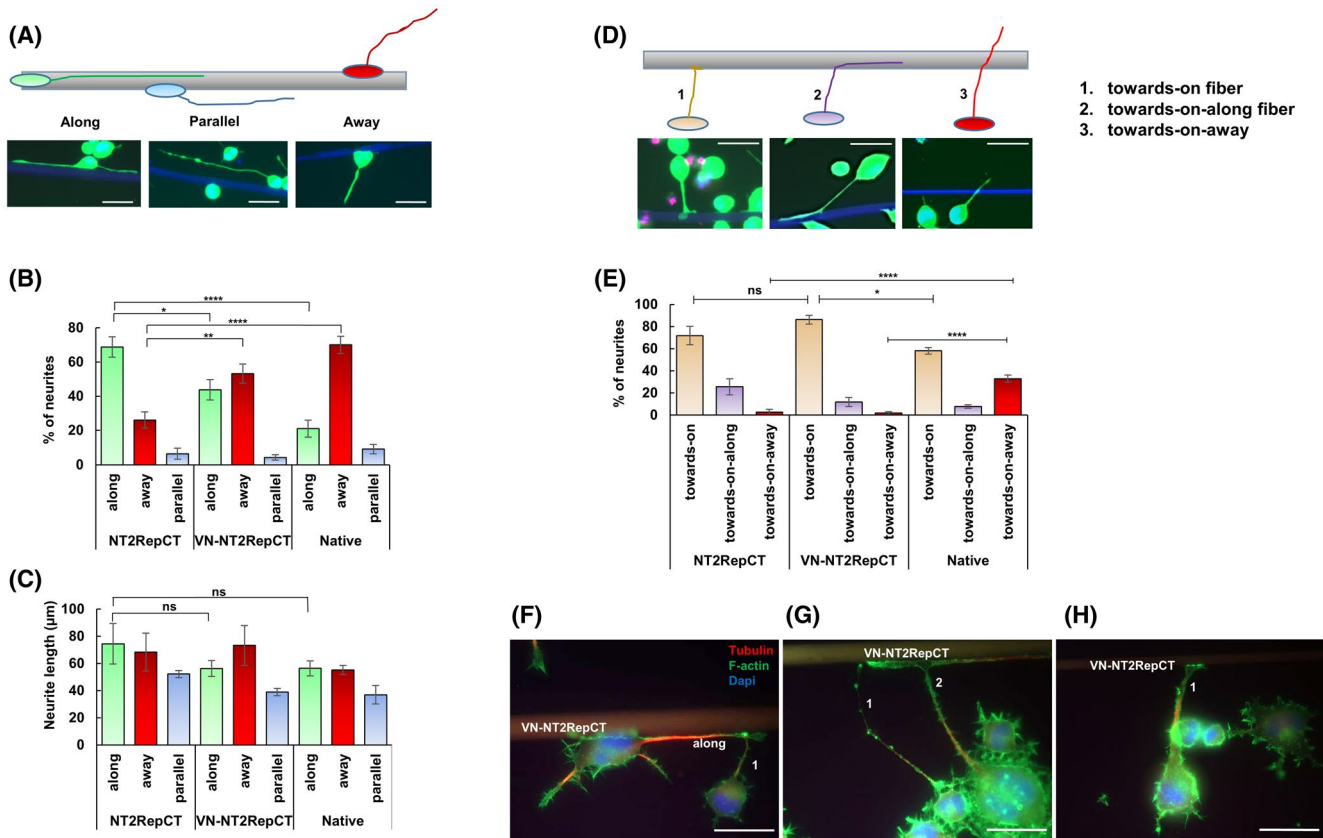


FIGURE 5 Neurite outgrowth on recombinant fibers NT2RepCT and VN-NT2RepCT as well as native dragline silk collected from *Larinioides scolopetarius*. Cells with their cell body attached to the fibers were analyzed for neurite guidance of the fibers by three different categories; neurites growing along, away from the fibers and parallel with the fibers (A). The percentage and the mean lengths of the longest neurite per cell for each category (B and C). NT2RepCT, VN-NT2RepCT, and native fibers were evaluated for neurite guidance properties by classifying neurites extending toward the fibers from cells that had their cell bodies located way from the fiber into three groups (1: toward-on, 2: toward-on along and 3: toward-on-away) (D, E). Examples from fluorescence images with merged channels and with 63× magnification of fixed ND7/23 cells differentiated on VN-NT2RepCT fibers for 48 h with 1 mM dbcAMP; fibers with cell body in contact with the fibers and the longest neurite growing along the fiber (F), having cell body not in contact but having its longest neurite growing towards on (1) (G and H) or towards-on-along (2) (G). F-actin (green), tubulin (red) and DAPI (blue). Scale bar: 50 µm. Data represent mean \pm SEM. NT2RepCT and VN-NT2RepCT and were performed in five independent experiments and native spider silks were analyzed from four independent experiments. ns, not significant, * $p < .05$ and **** $p < .0001$

These cells are often used as a surrogate for peripheral sensory neurons since they extend long neurites and differentiate into polarized cells after addition of nerve growth factor and/or dbcAMP.^{37,55–58} Moreover, differentiated ND7/23 cells express sensory neuron markers such as TrkA, Substance P, and CGRP,³⁷ which attest to their suitability for in vitro studies of peripheral nerve regeneration. We included several control substrates in order to benchmark the performance of NT2RepCT and VN-NT2RepCT matrices, that is, PDL as it is the recommended substrate for ND7/23, L111, and L511 that have been reported to be important ECM proteins for neurite sprouting of adult DRG in vitro¹⁴ and L521 that is present at neuromuscular junctions.^{59,60} Interestingly, ND7/23 cells proliferated and differentiated well on NT2RepCT and VN-NT2RepCT coatings, in fact none

of the investigated substrates alone or in combination outperformed the VN-NT2RepCT in cell survival and fraction neurite bearing cells. Cells that were cultured on NT2RepCT, VN-NT2RepCT, and PDL, respectively, developed neurites to a larger degree but the length of these neurites was shorter compared to cells cultured on L511 and L511 (Figure 2).

Based on these results, we tested if the VN-NT2RepCT could be further optimized as a matrix for neurite growth by adding laminins. Since VN-NT2RepCT and laminins require different coating procedures, we first coated the wells with VN-NT2RepCT which were dried and then different combinations of laminins were added on top. Analyses by Western Blot confirmed that laminins were present after coating on top of VN-NT2RepCT (Figure S3). None of these multicomponent coatings

outperformed VN-NT2RepCT in terms of cell survival and fraction neurite bearing cells. Only when a mixture of L511 and L521 was coated on top of VN-NT2RepCT, the neurite length was significantly longer compared to VN-NT2RepCT coatings.

Since both spider silk coatings behaved so well in all aspects investigated (i.e., cells survival, cell proliferation, and neurite growth), even compared to the laminin coatings, we spun fibers from NT2RepCT and VN-NT2RepCT, respectively. In this part of the study, we also included native dragline silk from *L. scolopariarius*, since dragline silk facilitates cell adhesion and neurite growth both in vitro and in vivo.^{23,24,38,61,62} For cells cultured on the three fiber types (NT2RepCT, VN-NT2RepCT, and native dragline silk), we found no significant differences in viability or mean length of neurites that grew along the fibers. However, another important parameter to consider is the potential of the fibers to guide neurites and to keep them from deviating from the direction of their intended target. Optimally, a nerve growth conduit should not only attract and enable nerve cells or their extending neurites to attach to the fiber material, but also support extensions of the neurites. Therefore we found it interesting to analyze if the different fibers varied regarding this aspect. The analyses were separated into cells attached to the fibers and the behavior of their extending neurites, and cell bodies not attached to the fibers, but with neurites extending toward and attaching to the fibers. We found that a larger fraction of the neurites from cells growing on NT2RepCT fibers were guided along the fiber compared to those growing on native spider silk. Surprisingly, this was true also when comparing the fraction of neurites growing along NT2RepCT fibers versus VN-NT2RepCT fibers, the reason for which remains to be determined. Analysis of the direction of neurites that were in physical contact with the fiber but without having their cell soma in contact with the fiber, showed that more neurites grew across and away from the native spider silk compared to recombinant spider silks. Taken together, our results indicate that both recombinant fiber types are suitable substrates for neurite extension, and that the recombinant silks may exceed native silks in term of guidance of neurite growth. One potential reason for this could be that the diameter of the fibers affects the neurite growth.^{55,62} However, analyses of the fiber diameter did not show any correlation between the diameter (ranging from 3 to 50 μm for recombinant silks and 3–7 μm for native silks) and the ability of the fibers to guide the neurites (Figure S4). Hence, there are most likely other explanations to why the recombinant fibers performed better than the native silk fibers, which remain to be investigated but could

be a result of differences in the protein composition between the fiber types, the presence of uncharacterized bioactive components in the fibers and the native fiber has a glycoprotein coat⁶³ which may influence the cells.

In this study we have shown that two types of spider silk proteins support growth and differentiation of a DRG neuron model cell line to the same degree as recombinant laminins and PDL. Furthermore, fibers made from these two proteins show equal or better performance for guiding neurites compared to native dragline silk, and thus, hold great potential for further development into NGCs.

ACKNOWLEDGMENTS

We thank Kerstin Nordling and Jenny Gustavsson (both from the Karolinska Institutet) for technical assistance. We are also thankful to Dr Lena Holm (Swedish University of Agricultural Sciences, Uppsala, Sweden) for valuable input on the manuscript. This work was supported by European Research Council (ERC) under the European Union's Horizon 2020 research and innovation program (grant agreement No 815357), the Center for Innovative Medicine (CIMED) at Karolinska Institutet and Stockholm City Council, Karolinska Institutet SFO Regen (FOR 4-1364/2019), and the Swedish Research Council (2019-01257) to AR.

DISCLOSURES

The authors declare no conflict of interest.

AUTHOR CONTRIBUTIONS

Magnus L. Hansson, Mattias K. Sköld, and Anna Rising designed the research; Magnus L. Hansson, Urmimala Chatterjee, Juanita Francis, Tina Arndt, and Christian Broman performed the experimental work; Magnus L. Hansson, Urmimala Chatterjee, Juanita Francis, Tina Arndt, Christian Broman, Jan Johansson, Mattias K. Sköld, and Anna Rising analyzed the data; Magnus L. Hansson, Urmimala Chatterjee, Juanita Francis, Mattias K. Sköld, and Anna Rising wrote the paper; and all authors read and approved the final manuscript.

ORCID

Magnus L. Hansson  <https://orcid.org/0000-0002-0983-3530>

Tina Arndt  <https://orcid.org/0000-0002-5190-0039>

Mattias K. Sköld  <https://orcid.org/0000-0001-6228-0691>

Anna Rising  <https://orcid.org/0000-0002-1872-1207>

REFERENCES

1. Scheib J, Höke A. Advances in peripheral nerve regeneration. *Nat Rev Neurol*. 2013;9:668-676.
2. Curcio M, Bradke F. Axon regeneration in the central nervous system: facing the challenges from the inside. *Annu Rev Cell Dev Biol*. 2018;34:495-521.

3. Mahar M, Cavalli V. Intrinsic mechanisms of neuronal axon regeneration. *Nat Rev Neurosci.* 2018;19:323-337.
4. Yiu G, He Z. Glial inhibition of CNS axon regeneration. *Nat Rev Neurosci.* 2006;7:617-627.
5. Houschyar KS, Momeni A, Pyles MN, et al. The role of current techniques and concepts in peripheral nerve repair. *Plast Surg Int.* 2016;2016:4175293.
6. Grinsell D, Keating CP. Peripheral nerve reconstruction after injury: a review of clinical and experimental therapies. *Biomed Res Int.* 2014;2014:698256.
7. Kanno H, Pearse DD, Ozawa H, Itoi E, Bunge MB. Schwann cell transplantation for spinal cord injury repair: its significant therapeutic potential and prospectus. *Rev Neurosci.* 2015;26:121-128.
8. Pabari A, Yang SY, Mosahebi A, Seifalian AM. Recent advances in artificial nerve conduit design: strategies for the delivery of luminal fillers. *J Control Release.* 2011;156:2-10.
9. Regas I, Loisel F, Haight H, Menu G, Obert L, Pluvy I. Functionalized nerve conduits for peripheral nerve regeneration: a literature review. *Hand Surg Rehabil.* 2020;39:343-351.
10. Meena P, Kakkar A, Kumar M, et al. Advances and clinical challenges for translating nerve conduit technology from bench to bedside for peripheral nerve repair. *Cell Tissue Res.* 2021;383:617-644.
11. Carvalho CR, Oliveira JM, Reis RL. Modern trends for peripheral nerve repair and regeneration: beyond the hollow nerve guidance conduit. *Front Bioeng Biotechnol.* 2019;7:337.
12. de Luca AC, Lacour SP, Raffoul W, di Summa PG. Extracellular matrix components in peripheral nerve repair: how to affect neural cellular response and nerve regeneration? *Neural Regen Res.* 2014;9:1943-1948.
13. Wallquist W, Patarroyo M, Thams S, et al. Laminin chains in rat and human peripheral nerve: distribution and regulation during development and after axonal injury. *J Comp Neurol.* 2002;454:284-293.
14. Plantman S, Patarroyo M, Fried K, et al. Integrin-laminin interactions controlling neurite outgrowth from adult DRG neurons in vitro. *Mol Cell Neurosci.* 2008;39:50-62.
15. Aumailley M, Bruckner-Tuderman L, Carter WG, et al. A simplified laminin nomenclature. *Matrix Biol.* 2005;24:326-332.
16. Mouw JK, Ou G, Weaver VM. Extracellular matrix assembly: a multiscale deconstruction. *Nat Rev Mol Cell Biol.* 2014;15:771-785.
17. Felding-Habermann B, Cheresch DA. Vitronectin and its receptors. *Curr Opin Cell Biol.* 1993;5:864-868.
18. Bergen K, Frödin M, von Gertten C, Sandberg-Nordqvist A, Sköld MK. Neurite growth and polarization on vitronectin substrate after in vitro trauma is not enhanced after IGF treatment. *Brain Sci.* 2018;8(8):151.
19. Otomo A, Ueda MT, Fujie T, et al. Efficient differentiation and polarization of primary cultured neurons on poly(lactic acid) scaffolds with microgrooved structures. *Sci Rep.* 2020;10:6716.
20. Melkounian Z, Weber JL, Weber DM, et al. Synthetic peptide-acrylate surfaces for long-term self-renewal and cardiomyocyte differentiation of human embryonic stem cells. *Nat Biotechnol.* 2010;28:606-610.
21. Varun D, Srinivasan GR, Tsai YH, et al. A robust vitronectin-derived peptide for the scalable long-term expansion and neuronal differentiation of human pluripotent stem cell (hPSC)-derived neural progenitor cells (hNPCs). *Acta Biomater.* 2017;48:120-130.
22. Salehi S, Koeck K, Scheibel T. Spider silk for tissue engineering applications. *Molecules.* 2020;25:737.
23. Kornfeld T, Nessler J, Helmer C, et al. Spider silk nerve graft promotes axonal regeneration on long distance nerve defect in a sheep model. *Biomaterials.* 2021;271:120692.
24. Radtke C, Allmeling C, Waldmann KH, et al. Spider silk constructs enhance axonal regeneration and remyelination in long nerve defects in sheep. *PLoS ONE.* 2011;6:e16990.
25. Petrou G, Jansson R, Höggqvist M, et al. Genetically engineered mucoadhesive spider silk. *Biomacromolecules.* 2018;19:3268-3279.
26. Wohlrab S, Müller S, Schmidt A, et al. Cell adhesion and proliferation on RGD-modified recombinant spider silk proteins. *Biomaterials.* 2012;33:6650-6659.
27. Bini E, Foo CW, Huang J, Karageorgiou V, Kitchel B, Kaplan DL. RGD-functionalized bioengineered spider dragline silk biomaterial. *Biomacromol.* 2006;7:3139-3145.
28. Widhe M, Johansson U, Hillerdahl CO, Hedhammar M. Recombinant spider silk with cell binding motifs for specific adherence of cells. *Biomaterials.* 2013;34:8223-8234.
29. Wu S, Johansson J, Damdimopoulou P, et al. Spider silk for xeno-free long-term self-renewal and differentiation of human pluripotent stem cells. *Biomaterials.* 2014;35:8496-8502.
30. Elsner MB, Herold HM, Müller-Herrmann S, Bargel H, Scheibel T. Enhanced cellular uptake of engineered spider silk particles. *Biomater Sci.* 2015;3:543-551.
31. Wu S, Johansson J, Hovatta O, Rising A. Efficient passage of human pluripotent stem cells on spider silk matrices under xeno-free conditions. *Cell Mol Life Sci.* 2016;73:1479-1488.
32. Stark M, Grip S, Rising A, et al. Macroscopic fibers self-assembled from recombinant miniature spider silk proteins. *Biomacromol.* 2007;8:1695-1701.
33. Andersson M, Jia Q, Abella A, et al. Biomimetic spinning of artificial spider silk from a chimeric minispidroin. *Nat Chem Biol.* 2017;13:262-264.
34. Arndt T, Laity PR, Johansson J, Holland C, Rising A. Native-like flow properties of an artificial spider silk dope. *ACS Biomater Sci Eng.* 2021;7:462-471.
35. Greco G, Francis J, Arndt T, et al. Properties of biomimetic artificial spider silk fibers tuned by PostSpin bath incubation. *Molecules.* 2020;25:3248.
36. Foelix RF. *Biology of Spiders.* Oxford University Press; 2011:136.
37. Jeon KI, Huxlin KR. How scars shape the neural landscape: key molecular mediators of TGF-beta1's anti-neuritogenic effects. *PLoS ONE.* 2020;15:e0234950.
38. Kornfeld T, Vogt PM, Bucan V, Peck CT, Reimers K, Radtke C. Characterization and Schwann cell seeding of up to 15.0 cm long spider silk nerve conduits for reconstruction of peripheral nerve defects. *J Funct Biomater.* 2016;7:30.
39. Li G, Chen K, You D, et al. Laminin-coated electrospun regenerated silk fibroin mats promote neural progenitor cell proliferation, differentiation, and survival in vitro. *Front Bioeng Biotechnol.* 2019;7:190.
40. White JD, Wang S, Weiss AS, Kaplan DL. Silk-tropoelastin protein films for nerve guidance. *Acta Biomater.* 2015;14:1-10.
41. Hu X, Wang X, Rnjak J, Weiss AS, Kaplan DL. Biomaterials derived from silk-tropoelastin protein systems. *Biomaterials.* 2010;31:8121-8131.
42. Rao F, Wang Y, Zhang D, et al. Aligned chitosan nanofiber hydrogel grafted with peptides mimicking bioactive brain-derived neurotrophic factor and vascular endothelial growth factor

- repair long-distance sciatic nerve defects in rats. *Theranostics*. 2020;10:1590-1603.
43. Yang S, Wang C, Zhu J, et al. Self-assembling peptide hydrogels functionalized with LN- and BDNF- mimicking epitopes synergistically enhance peripheral nerve regeneration. *Theranostics*. 2020;10:8227-8249.
44. Widhe M, Bysell H, Nystedt S, et al. Recombinant spider silk as matrices for cell culture. *Biomaterials*. 2010;31:9575-9585.
45. Aigner TB, Haynl C, Salehi S, O'Connor A, Scheibel T. Nerve guidance conduit design based on self-rolling tubes. *Mater Today Bio*. 2020;5:100042.
46. Uebersax L, Mattotti M, Papaloizos M, Merkle HP, Gander B, Meinel L. Silk fibroin matrices for the controlled release of nerve growth factor (NGF). *Biomaterials*. 2007;28:4449-4460.
47. Madduri S, Papaloizos M, Gander B. Trophically and topographically functionalized silk fibroin nerve conduits for guided peripheral nerve regeneration. *Biomaterials*. 2010;31:2323-2334.
48. Li H, Kuwajima T, Oakley D, et al. Protein prenylation constitutes an endogenous brake on axonal growth. *Cell Rep*. 2016;16:545-558.
49. Manoukian OS, Arul MR, Rudraiah S, Kalajzic I, Kumbar SG. Aligned microchannel polymer-nanotube composites for peripheral nerve regeneration: Small molecule drug delivery. *J Control Release*. 2019;296:54-67.
50. Zhang N, Milbreta U, Chin JS, et al. Biomimicking fiber scaffold as an effective in vitro and in vivo microRNA screening platform for directing tissue regeneration. *Adv Sci*. 2019;6:1800808.
51. Song J, Li X, Li Y, et al. Biodegradable and biocompatible cationic polymer delivering microRNA-221/222 promotes nerve regeneration after sciatic nerve crush. *Int J Nanomed*. 2017;12:4195-4208.
52. Landreh M, Andersson M, Marklund EG, et al. Mass spectrometry captures structural intermediates in protein fiber self-assembly. *Chem Commun*. 2017;53:3319-3322.
53. Otkovs M, Andersson M, Jia Q, et al. Degree of biomimicry of artificial spider silk spinning assessed by NMR spectroscopy. *Angew Chem Int Ed*. 2017;56:12571-12575.
54. Aggarwal N, Eliaz D, Cohen H, et al. Protein nanofibril design via manipulation of hydrogen bonds. *Commun Chem*. 2021;4:62.
55. Binder C, Milleret V, Hall H, Eberli D, Luhmann T. Influence of micro and submicro poly(lactic-glycolic acid) fibers on sensory neural cell locomotion and neurite growth. *J Biomed Mater Res B Appl Biomater*. 2013;101:1200-1208.
56. Haberberger RV, Barry C, Matusica D. Immortalized dorsal root ganglion neuron cell lines. *Front Cell Neurosci*. 2020;14:184.
57. Wood JN, Bevan SJ, Coote PR, et al. Novel cell lines display properties of nociceptive sensory neurons. *Proc Biol Sci*. 1990;241:187-194.
58. Wu D, Huang W, Richardson PM, Priestley JV, Liu M. TRPC4 in rat dorsal root ganglion neurons is increased after nerve injury and is necessary for neurite outgrowth. *J Biol Chem*. 2008;283:416-426.
59. Domogatskaya A, Rodin S, Tryggvason K. Functional diversity of laminins. *Annu Rev Cell Dev Biol*. 2012;28:523-553.
60. Patton BL, Miner JH, Chiu AY, Sanes JR. Distribution and function of laminins in the neuromuscular system of developing, adult, and mutant mice. *J Cell Biol*. 1997;139:1507-1521.
61. Millesi F, Weiss T, Mann A, et al. Defining the regenerative effects of native spider silk fibers on primary Schwann cells, sensory neurons, and nerve-associated fibroblasts. *FASEB J*. 2021;35:e21196.
62. Hafner K, Montag D, Maeser H, et al. Evaluating adhesion and alignment of dental pulp stem cells to a spider silk substrate for tissue engineering applications. *Mater Sci Eng C Mater Biol Appl*. 2017;81:104-112.
63. Augsten K, Mühlig P, Herrmann C. Glycoproteins and skin-core structure in *Nephila clavipes* spider silk observed by light and electron microscopy. *Scanning*. 2000;22:12-15.

SUPPORTING INFORMATION

Additional supporting information may be found online in the Supporting Information section.

How to cite this article: Hansson ML, Chatterjee U, Francis J, et al. Artificial spider silk supports and guides neurite extension in vitro. *FASEB J*. 2021;35:e21896. <https://doi.org/10.1096/fj.20210916R>